

Changes in Optic Nerve Head Blood Flow During Horizontal Ocular Duction

Manami Kawai,¹ Toshiaki Goseki,^{1,2} Kazunori Hirasawa,¹ Hitoshi Ishikawa,³ and Nobuyuki Shoji¹

¹Department of Ophthalmology, Kitasato University School of Medicine, Kanagawa, Japan

²Department of Ophthalmology, International University of Health and Welfare Atami Hospital, Shizuoka, Japan

³Department of Orthoptics and Visual Science, Kitasato University School of Allied Health Sciences, Kanagawa, Japan

Correspondence: Toshiaki Goseki, International University of Health and Welfare, 13-1 Higashi-kaigan-cho, Atami-City, Shizuoka 413-0012, Japan; goseki@iuhw.ac.jp

Received: June 3, 2023

Accepted: November 29, 2023

Published: January 3, 2024

Citation: Kawai M, Goseki T, Hirasawa K, Ishikawa H, Shoji N. Changes in optic nerve head blood flow during horizontal ocular duction. *Invest Ophthalmol Vis Sci.* 2024;65(1):7. <https://doi.org/10.1167/iovs.65.1.7>

PURPOSE. In this study, we aimed to compare blood flow changes in the optic nerve head (ONH) during horizontal ocular duction among normal, primary open-angle glaucoma (POAG), and normal-tension glaucoma (NTG) eyes.

METHODS. In this cross-sectional study, we included 90 eyes from 90 participants (30 control eyes, 30 POAG eyes, and 30 NTG eyes). ONH blood flow was measured with laser speckle flowgraphy using an external fixation light to induce central gaze, abduction, and adduction at 30 degrees for each eye. The mean blur rate (MBR) of the entire ONH area (MA), vascular region (MV), and tissue region (MT), and the change ratio were analyzed. The change ratio was defined as abduction or adduction value/central gaze value.

RESULTS. In the control group, MA significantly decreased during adduction (22.9 ± 3.7) compared with that during central gaze (23.6 ± 3.9 , $P < 0.05$). In the POAG group, MA (adduction = 17.4 ± 3.8 and abduction = 17.3 ± 3.6) and MV (adduction = 37.9 ± 5.6 and abduction = 38.0 ± 5.6) significantly decreased during adduction and abduction compared with those during central gaze (18.0 ± 4.1 and 39.5 ± 6.3 , respectively, $P < 0.05$). In the NTG group, MA significantly decreased during adduction (17.4 ± 4.2) compared with that during central gaze (18.1 ± 4.6) and abduction (18.1 ± 4.8 , $P < 0.05$). The change ratio did not differ between the glaucoma and control groups.

CONCLUSIONS. ONH blood flow decreased during horizontal ocular duction regardless of normal or glaucoma states; however, the change ratio was comparable between the normal and glaucoma groups.

Keywords: eye movements, blood flow, optic nerve head (ONH), glaucoma

The prevalence of glaucoma is approximately 5% in people aged over 40 years.^{1,2} Lowering intraocular pressure (IOP) has been established as an evidence-based glaucoma treatment. Most cases of glaucoma stop progressing when the IOP is lowered; however, some cases progress even when the IOP is lowered, and various factors other than IOP have been reported.³⁻¹⁰

Mechanical stress has been reported because the optic nerve (ON) is excessively flexed during ocular adduction compared with that during central gaze or abduction on magnetic resonance images.^{11,12} This is because the orbits are angled temporally, and the ON is inserted nasally into the orbit. Geometrically, the tension on the nerve is reduced during abduction because the nerve head is rotated nasally, allowing the ON to be more redundant. However, when the eye rotates during adduction from the central gaze position, the nerve head moves temporally in a larger arc, and the ON bends near the attachment between the globe and ON and the sheath to straighten. Additionally, due to the contraction of the medial rectus muscle, the mechanical load is applied to the globe by resistance force from not only the lateral

rectus muscle but also the ON and its sheath.¹¹ Morphological changes in the ON during this adduction are greater in primary open-angle glaucoma (POAG) eyes than in healthy eyes.^{12,13} Excessive adduction was speculated to be a cause of glaucoma progression, affecting axonal damage in the ON, lamina cribrosa (LC), and peripapillary tissues, including the sclera and globe morphology.

In addition, morphological changes of the optic nerve head (ONH) during horizontal ocular duction can be detected by optical coherence tomography (OCT). Normal eyes showed greater LC distortion during abduction and adduction¹⁴ and greater deformation of the ONH and peripapillary Bruch's membrane¹⁵ and the peripapillary choroid¹⁶ around the ONH during adduction than during abduction. The ONH and peripapillary vessels significantly deviated temporally during adduction and nasally during abduction.¹⁷ Although these reports have shown that horizontal ocular duction leads to morphological changes in the ON, ONH, peripapillary tissues, and vascular deviation, secondary changes to ON and ONH blood flow have not been studied. Eyes with glaucoma are reported to have



reduced ONH blood flow in central gaze compared with that in healthy eyes.^{18,19} Compression of the vascular pathway interferes with blood supply and cause tissue damage,^{20,21} which may further reduce blood flow with changes in ON and ONH morphology during both abduction and adduction.

In this study, we aimed to investigate the effects of horizontal ocular duction on ONH blood flow by measuring ONH blood flow with horizontal ocular duction and comparing these values in healthy and glaucoma eyes.

METHODS

This cross-sectional study was conducted after approval from the Kitasato University Ethics Committee (C20-367) in accordance with the Helsinki Convention. Informed consent was obtained from the participants after explanation of the study.

Data were obtained between April 2020 and March 2022. All eyes belonged to Japanese individuals. The criteria for the control group were the absence of glaucoma and within 21 mm Hg on the Goldmann applanation tonometer. Moreover, the criteria for glaucoma were glaucomatous changes in the ONH, visual field defects based on the Anderson-Patella classification, and glaucoma within 30 mm Hg on the Goldmann applanation tonometer. The patients with POAG had an IOP of ≥ 22 mm Hg before glaucoma treatment, and those with normal-tension glaucoma (NTG) had an IOP of ≤ 21 mm Hg at every visit. The glaucoma cases included two untreated patients. Previous glaucoma surgery included trabecular micro bypass stent use, selective laser trabeculoplasty, and trabeculectomy in one patient each.

The exclusion criteria common to the control and glaucoma groups were (1) corneal disease, retinal disease, strabismus or ocular motility disorder, severe dry eye, cataract Emery-Little classification 3 or higher, or an ophthalmologic disease affecting blood flow measurements other than refractive error; (2) cardiovascular disease or diabetes diagnosis; (3) systolic blood pressure (SBP) > 150 mm Hg and diastolic blood pressure (DBP) > 90 mm Hg; (4) medication affecting blood flow (Ca channel blockers, alpha-1/beta-1 blockers, and PDE5 inhibitors); (5) best corrected visual acuity better than LogMAR 0.1; (6) equivalent sphere of refraction $> \pm 8.00$ diopters (D) and axial length > 26.50 mm; and (7) history of ocular surgery (including refractive surgery or multifocal intraocular lens insertion) other than cataract or glaucoma surgery.

Laser Speckle Flowgraphy Measurement Methods

Laser speckle flowgraphy (LSFG-NAVI, Softcare Co. Ltd., Fukutsu, Japan) helps measure intraocular blood flow.²² LSFG-NAVI is a non-contact device used for quantitative measurement of blood flow in the ONH, choroid, retina, and iris in vivo using the speckle phenomenon induced by an 830-nm near-infrared laser. LSFG-NAVI parameters are the mean blur rate (MBR; in arbitrary units [AUs]), which is a quantitative index of blood flow velocity in the target tissues, and the relative blood flow index. The MBR had high reproducibility in previous reports,^{23,24} and it helps assess the severity of glaucoma as the MBR decreases with more severe glaucoma.^{18,25}

On the examination day, the participants were asked not to smoke or consume caffeine, and measurements were

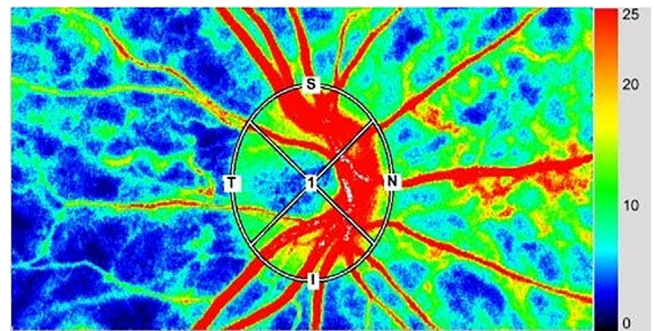


FIGURE 1. Measured results from the laser speckle flowgraphy false-color map and manually drawn optic nerve head-related rubber band. Higher values indicate faster blood flow, and warmer colors indicate areas of velocity. The measurement area is quadratically divided into S = superior, T = temporal, I = inferior, and N = nasal.

taken between 1:00 PM and 6:00 PM at least 2 hours after a meal. Because only one eye was tested, one eye was randomly selected if both met the recruitment criteria. The measurement protocol was as follows.

Tropicamide 0.4% (Mydrin-M; Santen Pharmaceutical Co., Ltd., Osaka, Japan) was used for mydriasis. After 30 minutes of medicine administration, the participant entered a dark room, and their blood pressure was measured. The head was fixed straight on the forehead pad of LSFG-NAVI, and the participant was asked to rest to ensure no movement. The participants fixated their non-measuring eyes on the external fixation light. The LSFG-NAVI angle was adjusted to maintain the measuring eye in the central gaze and the center of the ONH in the center of the image capture screen. Next, the external fixation light was adjusted to ensure a gaze angle of 30 degrees abduction or adduction for the measuring eye using a goniometer, and then, the LSFG gimbal was swung to center the ONH in the image. Fixation was monitored on the screen. The measured angle of the eye in this study was determined to be 30 degrees based on previous reports that the ONH and peripapillary Bruch's membrane¹⁵ are more deformed at 26 degrees or more and the peripapillary choroid of the ONH is more deformed at 35 degrees,¹⁶ considering the participant's limited ability to maintain ocular duction. The order of abduction and adduction was randomized, and measurements were taken after 2 minutes each time the eye position was changed. Data for central gaze, abduction, and adduction were measured three times each, and the average value was used. The ONH rubber band was determined using the LSFG-NAVI's View Angle 21 degrees, 750 × 360-pixel image. The analysis range was set manually with reference to the papillary shape of the color fundus photograph. The all-area MBR value (MA); the ONH vessel-area MBR (MV), which corresponds to the blood flow velocity through the large vessels; and the ONH tissue-area MBR (MT), which corresponds to microcirculation, were calculated by automatically averaging the data acquired using the software over a 4-second period. MA, MV, and MT were also calculated for the superior, temporal, inferior, and nasal quadrants of the entire rubber band (Fig. 1). Because the values obtained from LSFG-NAVI are relative blood flow indices and individual comparisons required correction,²⁶ the percent change was calculated as follows: change ratio = abduction or adduction value/central gaze value. In this study, only ONH blood flow evaluation was

performed because the reproducibility of ONH is better than that of retinal whole artery and whole vein analysis.²³

Disc area, cup area, and circumpapillary retinal nerve fiber layer (cp-RNFL) thickness were obtained from 3D-OCT Triton (Topcon, Tokyo, Japan). The β PPA was derived from Triton fundus photographs. The area of β PPA was calculated using ImageJ (US National Institutes of Health, Bethesda, MD, USA) after correction using the Littman's method.²⁷ Mean arterial blood pressure (MAP) and ocular perfusion pressure (OPP) were calculated as follows: MAP = DBP + 1/3 (SBP - DBP) and OPP = 2/3MAP-IOP.

Statistical Analysis

Data are presented as mean \pm standard deviation. Statistical analyses were performed using R (version 3.4.0; The Foundation for Statistical Computing, Vienna, Austria). The intraclass correlation coefficients of blood flow between the 2 examiners were calculated from 10 randomly selected participants. Within-group comparisons were performed using a paired *t*-test or Wilcoxon signed-rank test, and between-group comparisons were performed using Fisher's exact test, *t*-test, and Mann-Whitney *U* test with Bonferroni correction. A *P* value \leq 0.05 indicated a significant difference.

RESULTS

This study included 30 healthy eyes (control), 30 eyes with POAG, and 30 eyes with NTG of any severity. Table 1 summarizes the details of the participants in each group. The mean age of all participants was 65.8 \pm 10.9 years, and the male-to-female ratio was 37:53. Significant differences in IOP, cup area, β PPA area, and cp-RNFL thickness were found between the control and POAG/NTG groups (*P* < 0.01). The intraclass correlation coeffi-

cients of blood flow were 0.993 (95% confidence interval [CI] = 0.972–0.998) for MA, 0.963 (95% CI = 0.863–0.991) for MV, and 0.989 (95% CI = 0.959–0.997) for MT.

A comparison of central gaze, abduction, and adduction positions in each group is shown in Figure 2. In the control group, MA (central gaze = 23.6 \pm 3.9 [minimum 17.1–maximum 34.0], abduction = 23.2 \pm 3.9 [16.0–29.9], and adduction = 22.9 \pm 3.7 [15.9–30.0]) was significantly lower during adduction than during central gaze (*P* < 0.05). There was no difference in MV (central gaze = 42.4 \pm 5.4 [28.3–53.3], abduction = 42.5 \pm 5.7 [28.5–52.8], adduction = 41.4 \pm 4.8 [31.0–48.5]), and MT (central gaze = 12.2 \pm 2.4 [8.4–19.7], abduction = 12.2 \pm 2.4 [7.8–18.9], and adduction = 11.9 \pm 2.2 [8.5–18.8]) during central gaze, abduction, and adduction.

MA (central gaze = 18.0 \pm 4.1 [8.6–25.4], abduction = 17.3 \pm 3.6 [9.5–23.2], adduction = 17.4 \pm 3.8 [8.9–23.3]), and MV (central gaze = 39.5 \pm 6.3 [24.4–54.6], abduction = 38.0 \pm 5.6 [27.2–49.6], and adduction = 37.9 \pm 5.6 [26.3–49.0]) in the POAG group were lower during adduction and abduction than during central gaze (MA = *P* < 0.01, MV = *P* < 0.05). MT (central gaze = 9.1 \pm 2.6 [4.0–15.3], abduction = 9.3 \pm 2.4 [4.2–13.3], and adduction = 8.9 \pm 2.3 [4.4–13.9]) was lower during adduction than during abduction (*P* < 0.05). MA (central gaze = 18.1 \pm 4.6 [5.3–26.6], abduction = 18.1 \pm 4.8 [6.0–28.0], and adduction = 17.4 \pm 4.2 [6.6–26.6]) in the NTG group was lower during adduction than during central gaze and abduction (*P* < 0.05); however, there was no significant difference in MV (central gaze = 39.4 \pm 7.8 [14.3–53.3], abduction = 39.6 \pm 7.6 [21.7–54.1], and adduction = 39.1 \pm 7.7 [20.4–55.6]) and MT (central gaze = 9.4 \pm 2.3 [4.0–13.8], abduction = 9.7 \pm 2.4 [4.6–14.1], and adduction = 9.3 \pm 2.3 [4.6–14.9]). In addition, regarding the four quadrants (Fig. 3), MA in the control group was lower during adduction than during central gaze for

TABLE 1. Participants' Demographic and Ocular Data

	Control (n = 30)	POAG (n = 30)	NTG (n = 30)	P Value		
				Control vs. POAG	Control vs. NTG	POAG vs. NTG
Age (y)	64.9 \pm 10.2	64.7 \pm 12.9	67.7 \pm 9.4	1.00	0.81	1.00
Sex (male:female)	11:19	14:16	12:18	1.00	1.00	0.81
Eye with IOL implanted	8	9	10	1.00	1.00	1.00
IOP (mm Hg)	13.5 \pm 2.7	17.4 \pm 4.1	13.3 \pm 3.2	<0.01	1.00	<0.01
Visual acuity (LogMAR)	-0.06 \pm 0.05	-0.02 \pm 0.08	-0.04 \pm 0.06	0.06	0.56	0.80
Refraction (D)	-1.95 \pm 2.53	-2.29 \pm 2.36	-2.12 \pm 2.48	1.00	1.00	1.00
AL (mm)	24.3 \pm 1.2	24.4 \pm 1.3	24.8 \pm 1.2	1.00	0.22	0.81
Disc area (mm ²)	1.95 \pm 0.31	1.94 \pm 0.46	1.88 \pm 0.56	1.00	0.50	0.92
Cup area (mm ²)	0.74 \pm 0.43	1.53 \pm 0.49	1.51 \pm 0.57	<0.01	<0.01	1.00
β PPA area (mm ²)	0.44 \pm 0.59	0.85 \pm 0.44	1.19 \pm 0.78	<0.01	<0.01	0.41
24-2 MD (dB)	-	-14.13 \pm 7.99	-13.58 \pm 6.75	-	-	0.78
Total cp-RNFLT (μ m)	102.1 \pm 10.4	58.8 \pm 13.8	62.4 \pm 14.0	<0.01	<0.01	0.99
Superior cp-RNFLT (μ m)	124.2 \pm 14.6	68.0 \pm 19.9	77.6 \pm 22.3	<0.01	<0.01	0.25
Temporal cp-RNFLT (μ m)	80.8 \pm 12.6	53.6 \pm 16.0	51.6 \pm 15.9	<0.01	<0.01	1.00
Inferior cp-RNFLT (μ m)	131.0 \pm 19.5	64.5 \pm 22.9	62.8 \pm 22.1	<0.01	<0.01	1.00
Nasal cp-RNFLT (μ m)	72.6 \pm 17.0	49.2 \pm 13.5	57.6 \pm 14.0	<0.01	<0.01	0.07
SBP (mm Hg)	125.5 \pm 16.5	127.8 \pm 15.0	129.1 \pm 15.0	1.00	1.00	1.00
DBP (mm Hg)	75.2 \pm 8.8	77.7 \pm 9.2	74.5 \pm 10.4	0.49	1.00	0.80
Heartbeat (bpm)	72.7 \pm 10.1	69.6 \pm 9.0	68.1 \pm 10.4	0.65	0.24	0.81
Pulse pressure (mm Hg)	50.3 \pm 13.2	50.1 \pm 12.9	54.5 \pm 16.8	1.00	0.87	0.80
MAP (mm Hg)	91.9 \pm 10.2	94.4 \pm 9.7	92.7 \pm 9.4	1.00	1.00	1.00
OPP (mm Hg)	47.8 \pm 6.8	45.5 \pm 7.7	48.5 \pm 6.2	0.67	1.00	0.25

IOL, intraocular lens; IOP, intraocular pressure; AL, axial length; PPA, peripapillary atrophy; RNFLT, retinal nerve fiber layer thickness; MAP, mean arterial pressure; OPP, ocular perfusion pressure; SAP, systolic blood pressure; DBP, diastolic blood pressure.

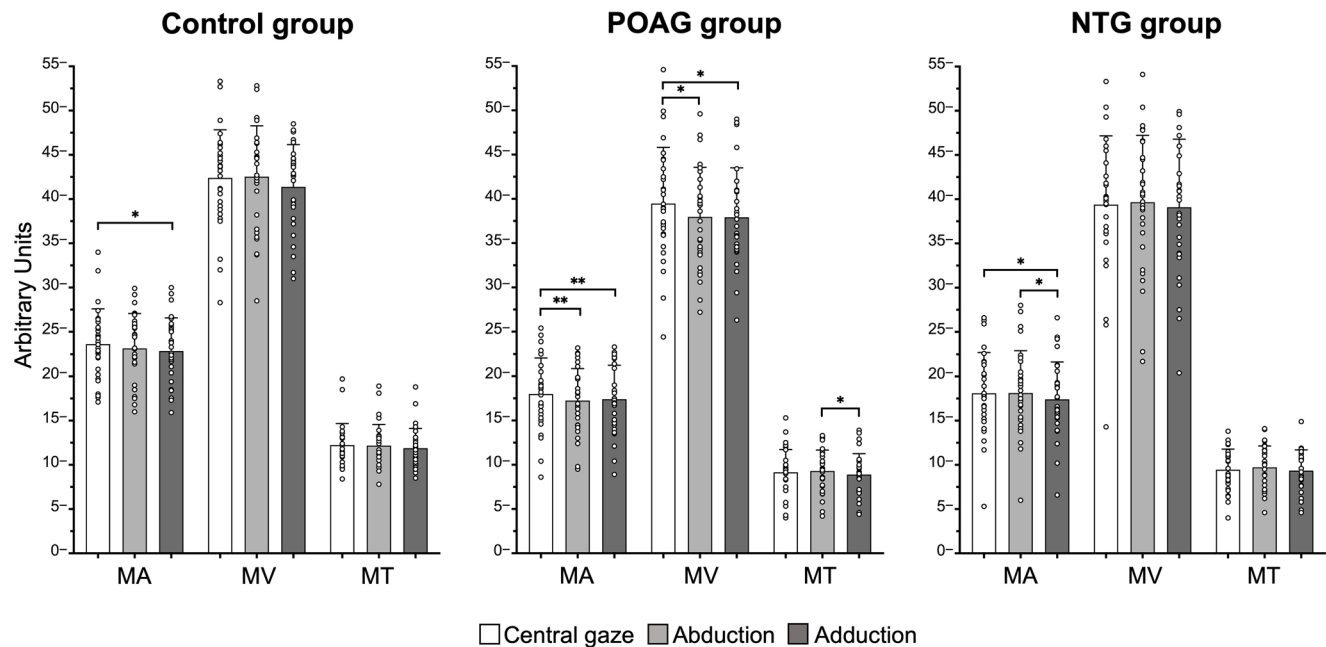


FIGURE 2. Comparison of blood flow during central gaze, abduction, and adduction in the control, POAG, and NTG groups (* $P < 0.05$, ** $P < 0.01$).

the superior, temporal, and inferior sides. The POAG group had lower MV on the superior and nasal sides during adduction and abduction than during central gaze and lower MV on the inferior sides during adduction. In addition, MT on the temporal side was lower during adduction than during abduction in all groups. Group comparisons of the change ratio in blood flow were not significantly different between the POAG and NTG groups compared with those in the control groups for both abduction and adduction (Table 2). Please refer to Supplementary Figure S1, which illustrates the change ratio distribution and Supplementary Table S2, which presents details regarding the reproducibility.

DISCUSSION

This study compared ONH blood flow during horizontal ocular duction, abduction, and adduction. In all groups (control, POAG, and NTG), ONH blood flow decreased during adduction compared with that during central gaze. In addition, the POAG group showed decreased blood flow in abduction. However, there was no difference in the change ratio in ONH blood flow among all the groups.

Simulations using finite element model during horizontal ocular duction showed that when ocular adduction reaches an angle that exhausts ON redundancy and the ON itself becomes a tether, reaction force to the contracting medial rectus muscle is applied to the globe by tension in the ON and its sheath.²⁸ Moreover, stress and strain are concentrated on the temporal side of the ONH and LC, regardless of the conditions of the IOP or intracranial pressure (ICP). On the other hand, the ON during abduction is redundant and sinuous, with a less mechanical load than that during adduction.¹²

The depth of laser speckle flowgraphy used in this study includes the LC.²⁹ The ONH vasculature³⁰ consists mostly of branches of the short posterior ciliary artery and a direct pathway through the ONH peripapillary choroid, with the

superficial nerve fiber layer and the posterior center of the LC being the retinal artery and vein. The LC connective tissues are anchored to a circumferential ring of collagen and elastin fibers^{31,32} in the peripapillary sclera through the wall of the optic canal. The short posterior ciliary artery flows through the sclera, and astrocyte-covered capillaries in the scleral portion pass through the LC. This septum bridging the scleral foramen serves to frame and support the microcirculatory vessels; the effect of peripapillary scleral distortion on the capillaries between the layers of the LC secondarily affects the volume flow through the scleral branch of the short posterior ciliary artery,³³ and the volume of the peripapillary choroid on the temporal side reduces by adduction pressure.¹⁶ This study hypothesized that mechanical compression of the short ciliary artery and choroidal vessels passing through the sclera and choroid deformed by adduction affects blood flow through the ONH during adduction in all groups, including healthy eyes. In addition, the ONH was divided into four quadrants, and the results showed that the temporal MT during adduction was lower than that during abduction in all groups. During adduction, the nasal sclera was almost unchanged, whereas the temporal sclera around the ONH was significantly deformed and thinned,³⁴ which may have affected the temporal ONH blood flow.

Blood flow in the POAG group relatively decreased during abduction and adduction compared with that during central gaze. The sclera significantly influences the IOP-induced strains on the LC, and the biomechanics of the ONH are strongly dependent on scleral characteristics.^{35,36} In contrast, the LC strain during horizontal ocular duction has been reported as particularly large during adduction and comparable to the strain when IOP increases significantly to 30 to 40 mm Hg, which is also significant during abduction.¹⁴ Therefore, we speculate that the combination of IOP and mechanical factors caused a relative decrease in blood flow in POAG eyes, both during adduction and abduction,

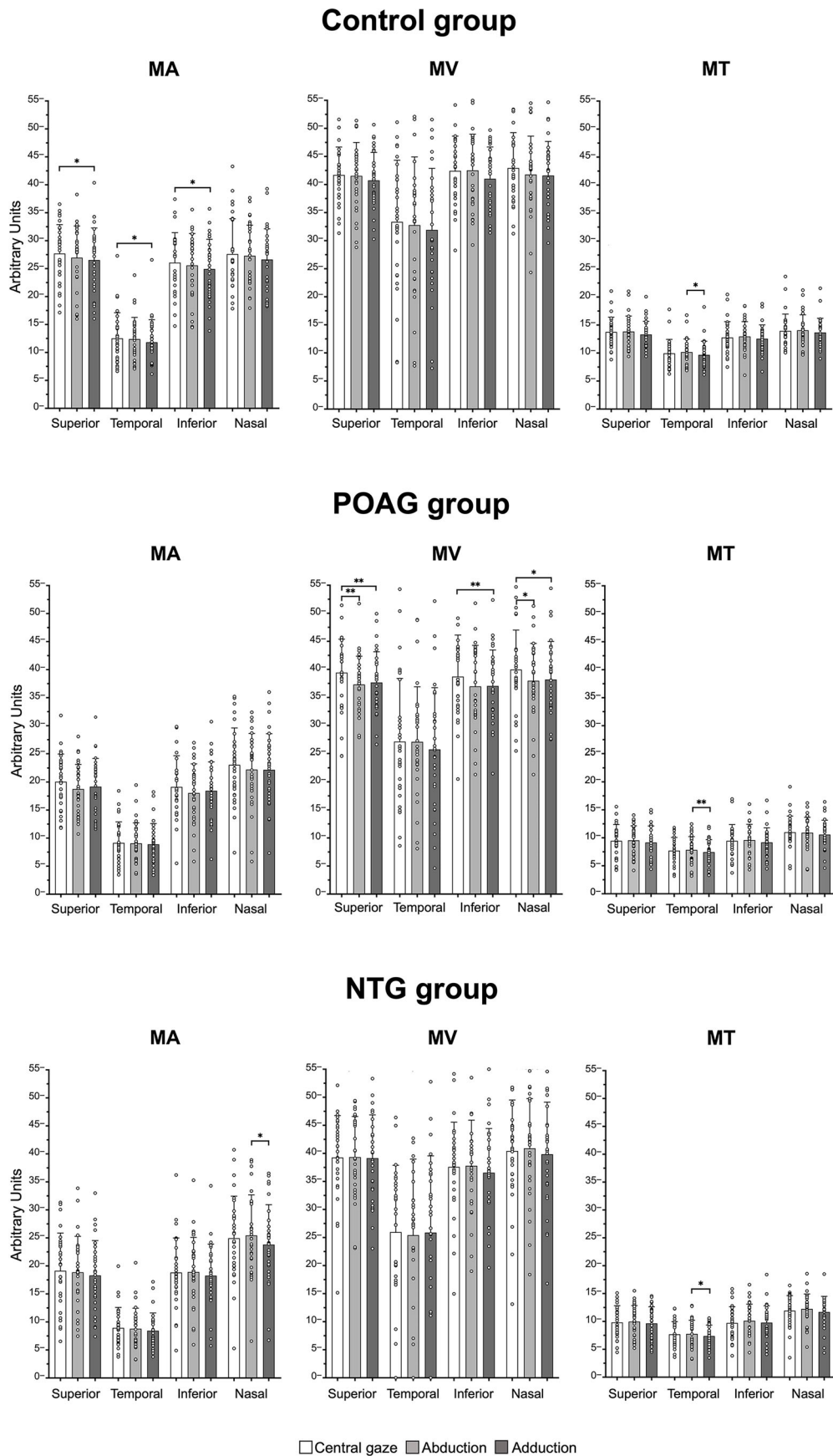


FIGURE 3. Comparison of blood flow during central gaze, abduction, and adduction when the optic nerve head is divided into quadrants in the control, POAG, and NTG groups (* $P < 0.05$, ** $P < 0.01$).

TABLE 2. Comparison of Change Ratio

	Control (n = 30)	POAG (n = 30)	NTG (n = 30)	P Value		
				Control vs. POAG	Control vs. NTG	POAG vs. NTG
Abduction						
MA	0.98 ± 0.08 (0.78–1.12)	0.96 ± 0.05 (0.86–1.10)	1.00 ± 0.06 (0.87–1.13)	0.96	0.68	0.03
MV	1.00 ± 0.08 (0.82–1.21)	0.97 ± 0.07 (0.84–1.12)	1.02 ± 0.12 (0.86–1.52)	0.15	1.00	0.10
MT	1.00 ± 0.08 (0.76–1.11)	1.02 ± 0.08 (0.85–1.17)	1.03 ± 0.08 (0.80–1.16)	0.72	0.36	1.00
Adduction						
MA	0.97 ± 0.06 (0.82–1.07)	0.97 ± 0.05 (0.87–1.07)	0.97 ± 0.08 (0.83–1.25)	1.00	1.00	1.00
MV	1.00 ± 0.09 (0.83–1.23)	0.97 ± 0.08 (0.82–1.14)	1.00 ± 0.12 (0.84–1.43)	1.00	1.00	0.76
MT	0.98 ± 0.06 (0.81–1.14)	0.98 ± 0.09 (0.82–1.14)	0.99 ± 0.10 (0.78–1.22)	1.00	1.00	1.00

due to the involvement of LC deformation caused by high IOP, a characteristic feature of POAG eyes.

The scleral characteristics have also been reported in relation to pathology. For instance, studies have reported no differences in scleral stress and strain between glaucomatous and healthy eyes,³⁷ as well as associations between posterior scleral thinning and increased IOP.³⁸ In addition, a link to ICP has traditionally been cited in the development and progression of glaucoma.^{39,40} This also affects mechanical stress during adduction and abduction. In a previous report, when IOP was high and ICP was low, the stress at the sclera and ON attachment of the ONH on the temporal side during adduction was higher than when it was normal.²⁸ Therefore, we assume that higher mechanical stress due to ICP states significantly affects blood flow in the LC. There have been reports of decreased sensitivity for adduction compared with that for abduction in visual field testing in the elderly.⁴¹ However, whether changes in blood flow due to horizontal ocular duction are a direct or indirect factor in glaucoma progression or deterioration of visual function is currently unknown and remains a matter for investigation.

This study had some limitations. First, glaucoma severity and treatment type were not the same among participants, and baseline data on IOP values were not collected before treatment. Because LC thickness correlates with blood flow and thicker LC correlates with higher MT values,⁴² the differences may depend on individual pathology. In addition to LC thickness, changes in choroid thickness, Bruch's membrane opening, and other structural markers of adduction-induced strain may account for individual variation. Whether changes in blood flow correlate with the degree of structural distortion in individual eyes and whether eyes with greater reductions in blood flow are more likely to develop glaucoma need to be examined in the future. Second, ONH ocular circulation has a static and dynamic autoregulatory capacity, which initiates in approximately 5 seconds in response to rapid IOP changes.²⁹ It is unclear whether autoregulation acts on horizontal ocular duction; however, this study did not consider the autoregulatory capacity⁴³ in the eyes. Generally, LSFG-NAVI is performed with the patient's gaze fixed in front or slightly shifted to capture images of the macula or ONH. Even a skilled certified orthoptist would face great difficulty in changing the patient's gaze horizontally by 30 degrees, changing the angle of the LSFG unit to capture the ONH in the center of the imaging screen in accordance with the visual axis, and focusing on the ONH each time. Therefore, measurement at a shorter time point (within 2 minutes) after eye movement was not practically possible in this study. Third, dorzolamide, a glaucoma eye

drop, increases ocular blood flow.^{44,45} Among the participants in this study, dorzolamide was used in one case in the POAG group and four cases in the NTG group. The blood flow measurement in the afternoon could not rule out the influence of dorzolamide, an ophthalmic solution administered three times a day. Last, abduction and adduction were only measured at 30 degrees as the measurement condition for this study, and it is unclear whether blood flow changes occur at higher angles of ocular duction.

In conclusion, we compared changes in ONH blood flow during horizontal ocular duction. Both healthy and glaucomatous eyes showed a relative decrease in blood flow during adduction when compared with that during central gaze. The change ratio in blood flow during horizontal ocular duction did not differ between healthy and glaucomatous eyes. These findings suggest that the observed changes in blood flow caused by ocular duction may not have significant clinical implications for the progression of glaucoma. However, the effects of ocular ductions involving larger angles or immediate and prolonged eye movements were not examined. Further investigation is warranted to determine whether changes in blood flow during ocular duction contribute to the onset and progression of glaucoma.

Acknowledgments

Supported by JSPS KAKENHI Grant Number JP20K09799.

Disclosure: **M. Kawai**, None; **T. Goseki**, None; **K. Hirasawa**, None; **H. Ishikawa**, Chugai Pharmaceutical Co., Ltd. (C), Alexion Pharmaceuticals, Inc. (C), Santen Pharmaceutical Co., Ltd. (C); **N. Shoji**, RE MEDICAL, Inc. (F)

References

- Iwase A, Suzuki Y, Araie M, et al. The prevalence of primary open-angle glaucoma in Japanese: the Tajimi Study. *Ophthalmology*. 2004;111(9):1641–1648.
- Yamamoto T, Iwase A, Araie M, et al. The Tajimi Study report 2: prevalence of primary angle closure and secondary glaucoma in a Japanese population. *Ophthalmology*. 2005;112(10):1661–1669.
- Suzuki Y, Iwase A, Araie M, et al. Risk factors for open-angle glaucoma in a Japanese population: the Tajimi Study. *Ophthalmology*. 2006;113(9):1613–1617.
- Tielsch JM, Katz J, Sommer A, Quigley HA, Javitt JC. Family history and risk of primary open angle glaucoma. The Baltimore Eye Survey. *Arch Ophthalmol*. 1994;112(1):69–73.
- Li Y, Mitchell W, Elze T, Zebardast N. Association between diabetes, diabetic retinopathy, and glaucoma. *Curr Diab Rep*. 2021;21(10):38.

6. Lin CC, Hu CC, Ho JD, Chiu HW, Lin HC. Obstructive sleep apnea and increased risk of glaucoma: a population-based matched-cohort study. *Ophthalmology*. 2013;120(8):1559–1564.
7. Almasieh M, Wilson AM, Morquette B, Cueva Vargas JL, Di Polo A. The molecular basis of retinal ganglion cell death in glaucoma. *Prog Retin Eye Res*. 2012;31(2):152–181.
8. Ernest PJ, Schouten JS, Beckers HJ, Hendrikse F, Prins MH, Webers CA. An evidence-based review of prognostic factors for glaucomatous visual field progression. *Ophthalmology*. 2013;120(3):512–519.
9. Leske MC, Heijl A, Hyman L, et al. Predictors of long-term progression in the early manifest glaucoma trial. *Ophthalmology*. 2007;114(11):1965–1972.
10. Sugisaki K, Inoue T, Yoshikawa K, et al. Factors threatening central visual function of patients with advanced glaucoma: a prospective longitudinal observational study. *Ophthalmology*. 2022;129(5):488–497.
11. Demer JL. Optic nerve sheath as a novel mechanical load on the globe in ocular duction. *Invest Ophthalmol Vis Sci*. 2016;57(4):1826–1838.
12. Demer JL, Clark RA, Suh SY, et al. Magnetic resonance imaging of optic nerve traction during adduction in primary open-angle glaucoma with normal intraocular pressure. *Invest Ophthalmol Vis Sci*. 2017;58(10):4114–4125.
13. Clark RA, Suh SY, Caprioli J, et al. Adduction-induced strain on the optic nerve in primary open angle glaucoma at normal intraocular pressure. *Curr Eye Res*. 2021;46(4):568–578.
14. Wang X, Beotra MR, Tun TA, et al. In vivo 3-dimensional strain mapping confirms large optic nerve head deformations following horizontal eye movements. *Invest Ophthalmol Vis Sci*. 2016;57(13):5825–5833.
15. Suh SY, Le A, Shin A, Park J, Demer JL. progressive deformation of the optic nerve head and peripapillary structures by graded horizontal duction. *Invest Ophthalmol Vis Sci*. 2017;58(12):5015–5021.
16. Chen JY, Le A, De Andrade LM, Goseki T, Demer JL. Compression of the choroid by horizontal duction. *Invest Ophthalmol Vis Sci*. 2019;60(13):4285–4291.
17. Le A, Chen J, Lesgart M, Gawargious BA, Suh SY, Demer JL. Age-dependent deformation of the optic nerve head and peripapillary retina by horizontal duction. *Am J Ophthalmol*. 2020;209:107–116.
18. Kiyota N, Kunikata H, Shiga Y, Omodaka K, Nakazawa T. Ocular microcirculation measurement with laser speckle flowgraphy and optical coherence tomography angiography in glaucoma. *Acta Ophthalmol*. 2018;96(4):e485–e492.
19. Shiga Y, Kunikata H, Aizawa N, et al. Optic nerve head blood flow, as measured by laser speckle flowgraphy, is significantly reduced in preperimetric glaucoma. *Curr Eye Res*. 2016;41(11):1447–1453.
20. Hayreh SS. The blood supply of the optic nerve head and the evaluation of it - myth and reality. *Prog Retin Eye Res*. 2001;20(5):563–593.
21. Hayreh SS. Blood supply of the optic nerve head and its role in optic atrophy, glaucoma, and oedema of the optic disc. *Br J Ophthalmol*. 1969;53(11):721–748.
22. Sugiyama T, Araie M, Riva CE, Schmetterer L, Orgul S. Use of laser speckle flowgraphy in ocular blood flow research. *Acta Ophthalmol*. 2010;88(7):723–729.
23. Aizawa N, Yokoyama Y, Chiba N, et al. Reproducibility of retinal circulation measurements obtained using laser speckle flowgraphy-NAVI in patients with glaucoma. *Clin Ophthalmol*. 2011;5:1171–1176.
24. Shiga Y, Asano T, Kunikata H, et al. Relative flow volume, a novel blood flow index in the human retina derived from laser speckle flowgraphy. *Invest Ophthalmol Vis Sci*. 2014;55(6):3899–3904.
25. Aizawa N, Kunikata H, Nakazawa T. Diagnostic power of laser speckle flowgraphy-measured optic disc microcirculation for open-angle glaucoma: analysis of 314 eyes. *Clin Exp Ophthalmol*. 2019;47(5):680–683.
26. Anraku A, Enomoto N, Tomita G, et al. Ocular and systemic factors affecting laser speckle flowgraphy measurements in the optic nerve head. *Transl Vis Sci Technol*. 2021;10(1):13.
27. Littmann H. Determination of the real size of an object on the fundus of the living eye. *Klin Monbl Augenheilkd*. 1982;180(4):286–289.
28. Park J, Shin A, Demer JL. Finite element modeling of effects of tissue property variation on human optic nerve tethering during adduction. *Sci Rep*. 2022;12(1):18985.
29. Liang Y, Fortune B, Cull G, Cioffi GA, Wang L. Quantification of dynamic blood flow autoregulation in optic nerve head of rhesus monkeys. *Exp Eye Res*. 2010;90(2):203–209.
30. Prada D, Harris A, Guidoboni G, Siesky B, Huang AM, Arciero J. Autoregulation and neurovascular coupling in the optic nerve head. *Surv Ophthalmol*. 2016;61(2):164–186.
31. Hernandez MR. Ultrastructural immunocytochemical analysis of elastin in the human lamina cribrosa. Changes in elastic fibers in primary open-angle glaucoma. *Invest Ophthalmol Vis Sci*. 1992;33(10):2891–2903.
32. Quigley HA, Dorman-Pease ME, Brown AE. Quantitative study of collagen and elastin of the optic nerve head and sclera in human and experimental monkey glaucoma. *Curr Eye Res*. 1991;10(9):877–888.
33. Langham ME. The temporal relation between intraocular pressure and loss of vision in chronic simple glaucoma. *Glaucoma*. 1980;2:427–435.
34. Shin A, Yoo L, Park J, Demer JL. Finite element biomechanics of optic nerve sheath traction in adduction. *J Biomech Eng*. 2017;139(10):1010101–10101010.
35. Sigal IA, Flanagan JG, Ethier CR. Factors influencing optic nerve head biomechanics. *Invest Ophthalmol Vis Sci*. 2005;46(11):4189–4199.
36. Sigal IA, Flanagan JG, Tertinegg I, Ethier CR. Modeling individual-specific human optic nerve head biomechanics. Part II: influence of material properties. *Biomech Model Mechanobiol*. 2009;8(2):99–109.
37. Coudrillier B, Tian J, Alexander S, Myers KM, Quigley HA, Nguyen TD. Biomechanics of the human posterior sclera: age- and glaucoma-related changes measured using inflation testing. *Invest Ophthalmol Vis Sci*. 2012;53(4):1714–1728.
38. Downs JC, Suh JK, Thomas KA, Bellezza AJ, Hart RT, Burgoyne CF. Viscoelastic material properties of the peripapillary sclera in normal and early-glaucoma monkey eyes. *Invest Ophthalmol Vis Sci*. 2005;46(2):540–546.
39. Berdahl JP, Allingham RR, Johnson DH. Cerebrospinal fluid pressure is decreased in primary open-angle glaucoma. *Ophthalmology*. 2008;115(5):763–768.
40. Berdahl JP, Fautsch MP, Stinnett SS, Allingham RR. Intracranial pressure in primary open angle glaucoma, normal tension glaucoma, and ocular hypertension: a case-control study. *Invest Ophthalmol Vis Sci*. 2008;49(12):5412–5418.
41. Shoji T, Mine I, Kumagai T, Kosaka A, Yoshikawa Y, Shinoda K. Age-dependent changes in visual sensitivity induced by moving fixation points in adduction and abduction using imo perimetry. *Sci Rep*. 2020;10(1):21175.
42. Omodaka K, Takahashi S, Matsumoto A, et al. Clinical factors associated with lamina cribrosa thickness in patients with glaucoma, as measured with swept source optical coherence tomography. *PLoS One*. 2016;11(4):e0153707.
43. Schmidl D, Garhofer G, Schmetterer L. The complex interaction between ocular perfusion pressure and ocular blood

- flow - relevance for glaucoma. *Exp Eye Res.* 2011;93(2):141–155.
44. Dong Y, Sawada Y, Cui J, et al. Dorzolamide-induced relaxation of isolated rabbit ciliary arteries mediated by inhibition of extracellular calcium influx. *Jpn J Ophthalmol.* 2016;60(2):103–110.
45. Avunduk AM, Sari A, Akyol N, et al. The one-month effects of topical betaxolol, dorzolamide and apraclonidine on ocular blood flow velocities in patients with newly diagnosed primary open-angle glaucoma. *Ophthalmologica.* 2001;215(5):361–365.